CHARACTERIZATION OF NICKEL-BASE SUPERALLOY
FRACTURE SURFACES BY AUGER ELECTRON SPECTROSCOPY

J.M. Walsh and N.P. Anderson

Pratt and Whitney Aircraft
Materials Engineering and Research Laboratory
East Hartford, Connecticut 06108

ABSTRACT

Auger electron spectroscopy (AES) was performed on a series
of impurity doped specimens of commercially pure nickel and
conventionally cast and directionally solidified nickel-base
superalloys in order to clarify the nature of certain trace
element effects that result in a reduction in the mechanical
properties. Since the trace element associated property
deterioration of the superalloys is mainly observed under load
at elevated temperatures, an experimental arrangement that more
closely simulates these conditions was devised for in situ AES
experiments. Direct evidence for the grain boundary segregation
of S, Bi, Te and Pb has been shown when the bulk levels were as
low as 40, 4.4, 6.8 and 10 ppm wt. while the elements Tl, Se,
Sn, Sb and As were not found at the grain boundaries. The
addition of Hf to the superalloy results in a significant
reduction in the amount of sulfur at the grain boundary. The
order in which the metallic trace elements segregate most
strongly to the grain boundaries correlates with previous work
which shows these elements to affect the mechanical properties
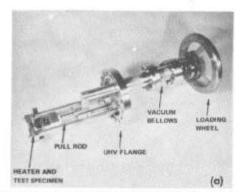in the same order.

INTRODUCTION

The deleterious effects of certain trace elements on the mechanical properties of nickel-base superalloys are now well known and documented (1). Several excellent studies correlating trace element levels of superalloys with tensile and creep rupture properties have been reported (2-4), however, the precise delineation of trace elements in the microstructure has received much less attention. Concentration of these trace elements in grain boundaries is generally thought to be responsible for embrittlement although little clear experimental evidence of these effects has been generated. This paper describes a two phase investigation involving the application of the Auger electron spectroscopy (AES) technique to clarify the nature of certain trace element effects in a series of nickel-base alloys. The first phase of the program consisted of the study of trace element effects in a simple system in the absence of aging precipitates or other second phases, i.e. commercially pure nickel with controlled additions of impurities. The second phase covered trace element behavior in superalloys.

The Auger spectroscopy technique provides for the compositional analysis of the top few atomic layers of solid sample surface and has gained wide acceptance over the past few years. Owing to this extreme surface sensitivity, the Auger method is especially suited for study of problems involving thin surface layers such as would be expected for a case of equilibrium grain boundary segregation of an impurity species.

EXPERIMENTAL PROCEDURE

Auger Instrumentation

A prerequisite for grain boundary study by AES is the existence of a measurable grain boundary surface. In materials that display intergranular embrittlement at room temperature or at least low grain boundary cohesive strength, an accepted method has been to fracture the material by impact in situ and perform AES on the resultant intergranular fracture surface. It is essential that the fracture be accomplished in the clean ultrahigh vacuum (UHV) system since adsorption of various species under ambient atmospheric conditions can easily mask any true grain boundary effects. High temperature structural materials such as superalloys often fail by grain boundary decohesion under service conditions, this being essentially a high temperature creep exposure, however, at room temperature these materials have relatively strong grain boundaries. In order to more closely simulate the service condition of the superalloy, a device has been designed and built that provides for the tensile mode loading and fracture of specimens at elevated temperatures in a Physical Electronics Industries Auger spectrometer. The fracture device is shown in Figure 1. The load is applied by taking up
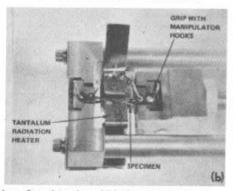

Figure 1: High temperature tensile device for in situ AES fracture study.

tension in a hand wheel threaded to a lead screw (Figure 1a). The lead screw drives a one inch diameter rod into the vacuum chamber through a flange mounted on a Varian flexible coupling. The load is transmitted from this main rod to the movable crosshead through a lever arm mechanism with a mechanical advantage of about 4/1. This arrangement easily fractures superalloy specimens with 0.125" diameter gage. Elevated temperature exposure is accomplished in a tantalum radiation heater that encloses the gage of the specimen (Figure 1b). After fracture, a vacuum manipulator picks up each half of the specimen by hooks attached to the grip and maneuvers it into the Auger analysis position.

Materials

Commercially Pure Nickel: The commercially pure nickel series contained the trace elements Pb, Bi, Te, Sb, Sn, As and Cu at bulk levels of up to about 25 ppm weight each. The alloys also contained up to 60 ppm weight S and 270 ppm weight C. The complete bulk analyses are given in Table I. The material was examined in the as cast condition. The specimens were fractured by impact at room temperature in the UHV system that had been baked out 8 hours @ 200°C and the resultant fracture surfaces were analyzed by AES. The fracture surfaces were also characterized in a scanning electron microscope. The depth distribution of any impurities found on the fracture surface was determined by monitoring the Auger signal of the element of interest while gently sputtering away material with a beam of argon ions.

Superalloys: The superalloys studied and their bulk trace element dopant levels are shown in Table II. Most of these specimens were fractured in situ in the tensile device described above. Two classes of superalloys were studied; conventionally cast and directionally solidified. Some of the alloys contained about 2 wt. pct. of the element Hf. In the case of the directionally solidified material, the tensile specimens were machined so that the stress axis was perpendicular to the solidification direction (Figure 2). The fractures were made at a temperature of about 1600°F which was estimated by using previously determined current and voltage settings required to bring a thermocouple instrumented specimen to 1600°F. The fracture program consisted

TABLE I

Bulk Chemical Analyses and AES Fracture
Surface Analyses of Doped Nickel

Element	Alloy 1		Alloy 2		Alloy 3	
	Bulk (ppm wt.)	Fracture Surface (at. pct.)	Bulk (ppm wt.)	Fracture Surface (at. pct.)	Bulk (ppm wt.)	Fracture Surface (at. pct.)
Bi	22	5	9	3	1	*
Te	26	0.5	8	*	1	*
Pb	26	*	8	*	1	*
Sb	21	*	8	*	1	*
Sn	24	*	9	*	2	*
As	30	*	10	*	10	*
Cu	15	*	15	*	15	*
S	50	28.5	60	35.5	40	21
C	65	*	210	*	270	7

* Not detected by AES

TABLE II

Bulk Chemical Analyses and AES Fracture Surface Analyses of Superalloys

	Alloy	Bi Bulk (ppm wt.)	Bi Fracture Surface Peak Ratio**	Te Bulk (ppm wt.)	Te Fracture Surface Peak Ratio	Pb Bulk (ppm wt.)	Pb Fracture Surface Peak Ratio	Tl Bulk (ppm wt.)	Tl Fracture Surface Peak Ratio	Se Bulk (ppm wt.)	Se Fracture Surface Peak Ratio	S Bulk (ppm wt.)	S Fracture Surface Peak Ratio
A	B-1900 + Hf	0.4	*	12.2	0.2	10	0.1	4.4	*	7.9	*	125	0.05
B	B-1900	4.4	0.15	6.8	0.1	13	0.05	1.8	*	0.6	*	30	0.2
C	B-1900	5.4	0.2	14.6	0.2	12	*	2.7	*	0.6	*	40	0.2
D	Directionally Solidified Mar M 200 + Hf	28	0.6	...	*	...	*	...	*	...	*	<20	0.02
E	B-1900 + Hf	...	*	...	*	2400	1.8	...	*	...	*	<20	0.03
F	Directionally Solidified Mar M 200 + Hf	...	*	...	*	160	0.5	...	*	...	*	<20	0.02

* not detected by AES

... element not added

** ratio of solute AES peak to Ni$_{848}$ peak after sensitivity adjustment using data from Reference 5.

130

of heating the specimen to ~1600°F and
then step-loading the specimen to
failure. The total time to failure
averaged about 3 hours. AES was
performed on both halves of each
fractured specimen. Depth profiles
were performed as described above. The
material and fracture surfaces were
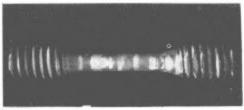also characterized by light and electron
metallography.

Figure 2: Transverse 1-1/2"
tensile specimen of directionally
solidified Mar M 200 + Hf.

RESULTS AND DISCUSSION

AES Experiments

Commercially Pure Nickel: All three of the alloys based on the commercially
pure nickel were fully embrittled in the as cast condition and provided
completely intergranular fracture surfaces (Figure 3) therefore the AES results
should reflect the grain boundary chemistry. Clear evidence was obtained for
grain boundary segregation of Bi, Te, S and in some cases, carbon. A typical
AES spectra for alloy No. 1 is shown in Figure 4 and indicates the presence of
Bi, Te and S in the grain boundary. The elements Pb, Sb, Sn, As and Cu were
not detected in the grain boundary. The AES results for all specimens are
given in Table I. The composition estimates were made by an accepted procedure
of relating peak-to-peak heights in the derivative Auger spectra to the
relative sensitivity of the Auger transitions for the pure elements (5).
Sputter-depth profiles were performed for the segregating species and indicated
that the solutes were confined to a narrow
zone in the vicinity of the grain boundary.
Typical sputter-depth profiles for bismuth
are shown in Figure 5.

The virgin fracture surfaces of all but
the highest bulk carbon level specimens
were free of carbon and oxygen. The
fracture surface of the alloy with 270 ppm
wt. bulk carbon contained carbon but no
oxygen suggesting a genuine segregation of
carbon within the alloy. A set of sputter-
depth profiles for S and C on the 3 alloys
is shown in Figure 6. These data clearly
show the strong grain boundary segregation
of S in all 3 alloys and the carbon
segregation which occurs only in alloy
No. 3. A gradual carbon buildup is
observed during sputtering. This is
commonly observed in sputtering experi-
ments and is simply adsorption of
residual carbon from the UHV system on the
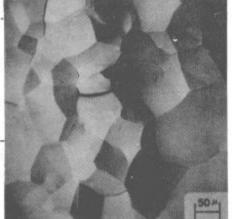very active sputtered surface.

Figure 3: SEM of intergranular
fracture surface of doped nickel
alloy No. 1.

The segregation of sulfur to nickel grain boundaries is a well known effect
(1, 6, 7) and has been recently confirmed by several AES workers (8, 9). The
current AES observations of sulfur segregation support these previous studies.
In practical engineering alloys, sulfur can be rendered significantly less
troublesome than the other trace elements because of the effectiveness of
elements such as Mn, Hf, Ti and La in lowering the sulfur activity (1, 10).

A number of studies have been made of the effect of the other metallic trace
elements on the mechanical properties of nickel-base alloys (2-4). These
studies indicate that of the current group of elements, Bi is the most damaging
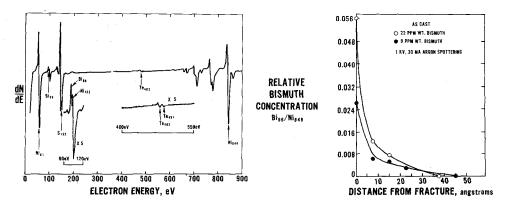followed in order of decreasing harmfulness by Te and Pb. An abrupt drop in

Figure 4: Auger spectra of virgin fracture surface of nickel alloy No. 1
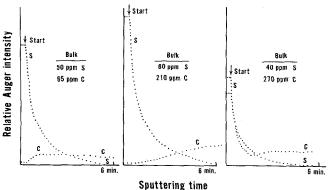
Figure 5: Bismuth sputter-depth profiles for nickel alloys No. 1 and 2.
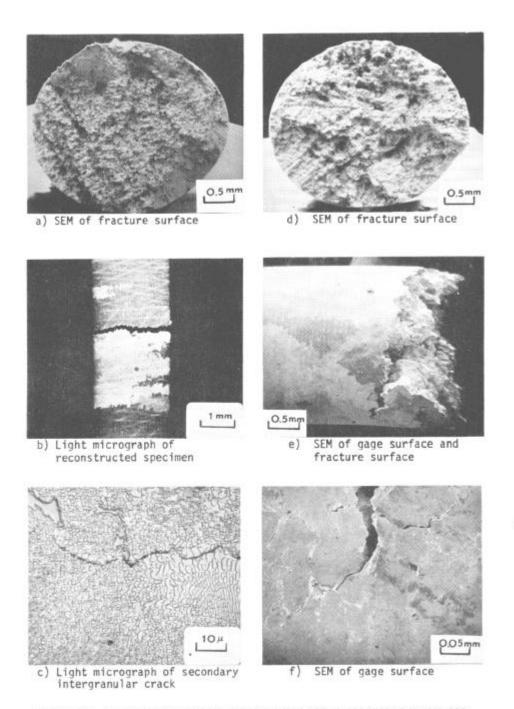
the damage effect occurs between Te and Pb while the elements, Sb, Sn, As and Cu were far less harmful. An interesting correlation can be drawn between the current AES results and these previous mechanical property studies. Bismuth, the trace metal that shows the highest interfacial activity, i.e. segregates most strongly to the grain boundary is indeed the same element that produces the most deleterious mechanical property effect. The second most harmful element, Te, is also grain boundary active but to a lesser extent than Bi. The elements Pb, Sb, Sn, As and Cu were not found at the grain boundaries in this experiment. This simply means that their concentrations at the fracture surface are below the AES minimum detectability limit of ~0.5-1 atomic percent. Some of these elements may and probably do segregate, however, the grain boundary/bulk enrichment ratios are probably less than for Bi and Te so that at the prevailing bulk levels a grain boundary concentration sufficient to measure does not build up. Carbon also exhibits interfacial activity but to a lesser extent than the Bi, Te and S since it was only observed when the bulk carbon level was 270 ppm weight.

Since the concentration of each of the metallic trace elements in the 3 alloys ranged from ~1 to 25 ppm weight while the sulfur concentration remained relatively constant (~40-60 ppm wt.) and yet all 3 alloys were fully embrittled, the embrittlement must be attributed to the saturation of grain boundaries by sulfur.

Superalloys: The superalloy fracture experiments resulted in fracture surfaces of a very dendritic character which were to a large extent intergranular. Examples of fractures for conventional and directionally solidified material

Figure 6: S and C simultaneous sputter-depth profiles for nickel alloys No. 1, 2 and 3.

Sputtering time

132

a) SEM of fracture surface

d) SEM of fracture surface

b) Light micrograph of
   reconstructed specimen

e) SEM of gage surface and
   fracture surface

c) Light micrograph of secondary
   intergranular crack

f) SEM of gage surface

Figure 7: Fractured specimens of directionally solidified Mar-M 200
+ Hf (a, b, c) and conventionally cast B-1900 (d, e, f) illustrating
intergranular nature of fractures.

are shown in Figure 7. Depending on bulk solute content, clear evidence was obtained for the grain boundary segregation of Bi, Te, Pb and S. Typical AES spectra for alloys A and B are given in Figure 8. The trace element grain boundary effects are summarized in Table II in terms of Auger peak height ratios relative to the Ni_{848} signal. The fractures were generally quite clean with regard to contaminants normally encountered from ambient atmospheric exposure. A small oxygen and small to moderate carbon peak was observed on each specimen. The shape and structure of the carbon peak was characteristic of metal carbides and is therefore attributed to the metal carbides which are known to be present at the grain boundaries of these materials. The external gage surface of each of the specimens was also examined by AES. The characteristics of the gage surfaces of most of the specimens were that they showed much stronger oxygen than the fracture, a much stronger carbon signal with peak structure more typical of amorphous carbon rather than metal carbide, stronger sulfur and no trace metals.

Sputtering experiments indicated that in most cases the segregants were confined to the top atomic layers as was the case for the doped nickel series. An exception to this behavior was the alloy containing 2400 ppm Pb; this material showed a preferential Pb concentration at the freshly fractured surface which decayed rapidly upon sputtering to a non-zero level which persisted throughout the sputter experiment. This observation suggests that Pb is present as a thin grain boundary film as well as in some other more generally distributed form which will be discussed further under microstructure.

Of the metallic solutes, Bi was the most strongly segregated followed by Te and then Pb. This behavior correlates well with the results on the doped nickel series described previously. Furthermore, a clear correlation can be made between these AES observations and the previously referenced studies relating trace elements with superalloy mechanical properties; the trace metals which have the most harmful effect upon the mechanical properties are the elements that segregate most strongly to the grain boundaries.

The elements Tl and Se were not detected at the grain boundaries when bulk levels were as high as 4.4 and 7.9 ppm weight respectively although these metals have certain properties characteristic of the confirmed interfacially active species including large atomic size relative to nickel, low solid solubility and low heat of sublimation. These elements then must have a lower grain boundary/bulk enrichment ratio.

Confirmation of grain boundary segregation of sulfur was reported earlier in this study for the case of commercially pure nickel. While grain boundary
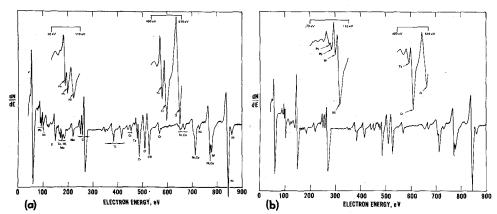

Figure 8: Auger spectra of intergranular fracture surfaces of (a) B-1900 + Hf, alloy A and (b) B-1900, alloy B.

segregation of sulfur was also observed in the superalloys, the extent was largely dependent upon the bulk Hf content which is an element known to be effective in improving superalloy ductility (11). A large sulfur segregation effect was observed in the Hf-free B-1900 (Table II) while the grain boundary sulfur level was much lower in the B-1900 containing ~2 w/o Hf.

Microstructural Observations

The materials were characterized by light and electron metallography in addition to the AES experiments. In the case of the alloys based on the commercially pure nickel, no evidence of a second phase grain boundary precipitate could be found either by SEM of virgin intergranular fracture surfaces or transmission electron microscopy and selected area electron diffraction of thin foils. The segregation effects observed, then, are likely of the elemental form.

The superalloy microstructures were studied carefully in the electron microprobe for evidence of Pb, Bi, Te and S. The elements Te and Bi could never be found in the microstructure. In the Hf-containing alloys, the sulfur was found only in a complex carbo-sulfide phase of the M_2SC type where the M component is hafnium-rich but also includes Zr and Ti. This constituent was confined primarily to gamma-gamma prime eutectic regions (Figure 9). At the higher bulk Pb levels (2400 ppm wt.), Pb was detected in the microstructure. It was not found as a continuous grain boundary phase but was confined to a discrete constituent at the periphery of the eutectic pools (Figure 10). X-ray energy spectroscopy (XES) analysis of the Pb-rich constituent extracted from a room temperature impact fracture surface (Figure 11) has indicated that it is essentially free Pb.

An explanation for the fact that Sn is less damaging to mechanical properties than most of the other metallic solutes (12) and also has lower interface activity can be given by its relatively higher solubility in the gamma-gamma prime eutectic compared to the other trace metals. Electron microprobe analysis of Hf modified B-1900 with a bulk Sn level of ~1000 ppm weight has shown that the only measurable Sn concentration (~0.3 w/o) is confined to the eutectic (Figure 12).
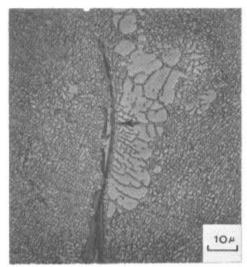

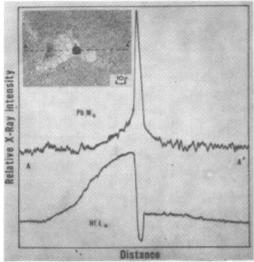Figure 9: M_2SC phase (arrow) in B-1900 + Hf.

Figure 10: Pb and Hf concentration profiles across eutectic in B-1900 + Hf containing 2400 ppm Pb.
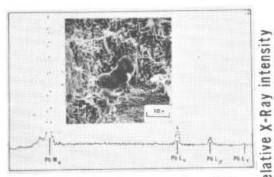
Figure 11: XES identification of Pb constituent extracted from fracture surface of B-1900 + Hf containing 2400 ppm Pb.
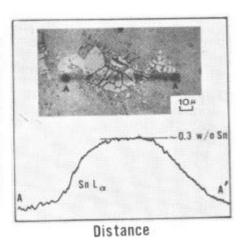

Figure 12: Sn concentration profile across eutectic in B-1900 + Hf with ~1000 ppm Sn.

SUMMARY

Direct evidence for grain boundary segregation of S, Bi, Te and Pb in nickel and nickel-base superalloys has been produced by Auger electron spectroscopy when the bulk levels were as low as 40, 4.4, 6.8 and 10 ppm weight respectively. The elements Tl, Se, Sn, Sb and As could not be found at the grain boundaries when the bulk levels were as high as 4.4, 7.9 21 and 30 ppm weight, respectively and this may be due to a lower grain boundary/bulk enrichment ratio or in the case of Sn in a superalloy, a higher solubility in the gamma-gamma prime eutectic. The addition of Hf to a superalloy causes a significant reduction in the amount of sulfur in the grain boundary. No specific micro-constituent could be associated with the Te and Bi however at the higher bulk Pb levels a globular constituent of essentially free Pb was detected at the eutectic periphery. The order in which the metallic trace elements segregate most strongly to the grain boundaries is the same order in which these elements affect the superalloy mechanical properties.

REFERENCES

1. C.G. Bieber and R.F. Decker: Trans. TMS-AIME, 1961, Vol. 221, p. 629.
2. D.R. Wood and R.M. Cook: Metallurgia, March 1963, p. 109.
3. R.J. Henricks and M.L. Gell: "Trace Element Effects in Cast Nickel-Base Superalloys", ASM Materials Engineering Congress, Chicago, Ill., 1973.
4. W.B. Kent: J. Vac. Sci. Technol, 1974. Vol. 11, p. 1038.
5. P.W. Palmberg, G.E. Riach, R.E. Weber and N.C. MacDonald: "Handbook of Auger Electron Spectroscopy", Physical Electronics Industries, Inc., 1972.
6. P.D. Merica and R.G. Waltenberg: "Malleability and Metallography of Nickel", Technologic Papers of the Bureau of Standards, 2 April 1925, Vol. 19, Paper No. 281, p. 155.
7. K.M. Olsen, C.F. Larkin and P.H. Schmitt: Trans. ASM, 1961, 53, p. 349.
8. A.W. Thompson: "Grain Boundaries in Engineering Materials", J. Walter, J. Westbrook and D. Woodford, eds., p. 607, Claitor's, Baton Rouge, 1975.
9. W.C. Johnson, J.E. Doherty, B.H. Kear and A.F. Giamei: Scripta Met., 1974, Vol. 8, p. 971.
10. A.F. Giamei and F.L. VerSnyder: "Grain Boundaries in Engineering Materials", J.L. Walter, J.H. Westbrook and D.A. Woodford, eds., p. 3, Claitor's, Baton Rouge, 1975.
11. D.N. Duhl and C.P. Sullivan: J. Met., 1971, Vol. 23, p. 38.
12. R.T. Holt and W. Wallace: "Impurities and Trace Elements in Nickel-Base Superalloys", Nat. Res. Council Canada Report No. LTR-ST. 760, 1975.